EBioMedicine 25 (2017) 143–153

Contents lists available at ScienceDirect

EBioMedicine

journal homepage: www.ebiomedicine.com

Research Paper

D-Ribose as a Contributor to Glycated Haemoglobin

Xixi Chen [a,1], Tao Su [a,1], Yao Chen [b], Yingge He [a], Ying Liu [a], Yong Xu [b], Yan Wei [a,c,*], Juan Li [c], Rongqiao He [a,c,d,*]

[a] State Key Laboratory of Brain and Cognitive Science, Institute of Biophysics, University of Chinese Academy of Sciences, Beijing 100101, China
[b] Southwest Medical University, Luzhou, Sichuan 646000, China
[c] CAS Key Laboratory of Mental Health, Institute of Psychology, University of Chinese Academy of Sciences, Beijing 100101, China
[d] Alzheimer's Disease Center, Beijing Institute for Brain Disorders, Capital Medical University, Beijing 100069, China

ARTICLE INFO

Article history:
Received 24 August 2017
Received in revised form 28 September 2017
Accepted 2 October 2017
Available online 5 October 2017

Keywords:
D-ribose
HbA1c
Type 2 diabetes mellitus
Transketolase
Benfotiamine

ABSTRACT

Glycated haemoglobin (HbA1c) is the most important marker of hyperglycaemia in diabetes mellitus. We show that D-ribose reacts with haemoglobin, thus yielding HbA1c. Using mass spectrometry, we detected glycation of haemoglobin with D-ribose produces 10 carboxylmethyllysines (CMLs). The first-order rate constant of fructosamine formation for D-ribose was approximately 60 times higher than that for D-glucose at the initial stage. Zucker Diabetic Fatty (ZDF) rat, a common model for type 2 diabetes mellitus (T2DM), had high levels of D-ribose and HbA1c, accompanied by a decrease of transketolase (TK) in the liver. The administration of benfotiamine, an activator of TK, significantly decreased D-ribose followed by a decline in HbA1c. In clinical investigation, T2DM patients with high HbA1c had a high level of urine D-ribose, though the level of their urine D-glucose was low. That is, D-ribose contributes to HbA1c, which prompts future studies to further explore whether D-ribose plays a role in the pathophysiological mechanism of T2DM.

1. Introduction

Type 2 diabetes mellitus (T2DM) is the most common type of diabetes mellitus and is characterized by hyperglycaemia (Trujillo et al., 2013) and insulin resistance (Reaven, 1988). Many diabetic patients develop acute or chronic complications, including blood vessels, brain, kidney, and liver damage (Nathan, 1993). Glycated haemoglobin A1c (HbA1c), resulting from an abnormally high level of reduced monosaccharides (such as D-glucose and D-ribose), is a factor in these complications (Chou et al., 2009; Huang et al., 2015; Sherwani et al., 2016). Both D-ribose and D-glucose react with haemoglobin (Hb), thus yielding HbA1c (Huisman et al., 1958; Koenig et al., 1976), which is the most important biomarker for chronic hyperglycaemia (Berg, 2013). As an active reducing monosaccharide, D-ribose reacts with amino acids, peptides and proteins, and produces glycated derivatives much more rapidly than D-glucose (Chen et al., 2009; Wei et al., 2009). The link between blood D-glucose and HbA1c has been intensively studied (Makris and Spanou, 2011); however, whether D-ribose is involved in the glycation of Hb and the subsequent production of HbA1c in diabetic patients is still not fully clarified and therefore requires further investigation.

2. Materials and Methods

2.1. Materials

D-ribose, D-glucose and benfotiamine (benzenecarbothioic acid, S-[2-[[(4-amino-2-methyl-5-pyrimidinyl) methyl] formylamino]-1-[2-(phosphonooxy)ethyl]-1-propen-1-yl]ester) were purchased from Sigma (St. Louis, Missouri). 4-(3-methyl-5-oxo-2-pyrazolin-1-yl) benzoic acid was purchased from J&K Scientific (Beijing, China).

2.2. Subject Enrolment

Patients with T2DM (n = 82, between 50 and 83 years old) were recruited from the Jianheng Diabetes Hospital, Beijing. Age-matched community-dewelling healthy subjects (n = 41) were used as controls, and their physical examinations were performed by the Medical Examination Center of the Third Hospital of Peking University. Informed consents were obtained from all participants. Subjects with T2DM conformed to the classification scheme and diagnostic criteria for DM as published in a report from an international expert committee. Their personal information and medical history were recorded in details. According to the diagnosis of diabetes recommended by the WHO, the patients were divided into two groups on the basis of their HbA1c levels: group 1 (6.5% (48 mmol/mol) ≤ [HbA1c] < 8.0% (64 mmol/mol)), and group 2 (HbA1c ≥ 8.0% (64 mmol/mol)). The patients were excluded if they were tested positive for urine proteins. To ensure the accuracy of sample analysis and to avoid protein interference, middle stream

* Corresponding authors at: State Key Laboratory of Brain and Cognitive Science, Institute of Biophysics, Chinese Academy of Sciences, 15 Datun Road, Chaoyang District, Beijing 100101, China.
E-mail addresses: yanwei@ibp.ac.cn (Y. Wei), herq@ibp.ac.cn (R. He).
[1] These authors contributed equally to this work.

https://doi.org/10.1016/j.ebiom.2017.10.001

morning urine was collected from subjects before their breakfast. The participants were instructed to avoid consuming high-fat diets and sugar one week before the samplings. Beverages such as wine and alcohol were forbidden the day before sampling. Prior to analysis, the samples were stored in a sealed sterile container at −80 °C. This study was approved by the ethics committee of the Institute of Biophysics, Chinese Academy of Sciences (2014-HRQ-1).

2.3. Data Availability

This trial was registered with the Chinese Clinical Trial Registry (ChiCTR), which was granted by the WHO International Clinical Trial Registration Platform (WHO ICTRP). The trial number is ChiCTR-RCS-14004437 (http://www.chictr.org/cn/).

2.4. Measurements of Urine D-ribose and D-glucose by UV-HPLC

Analyses of urine D-ribose and D-glucose were performed in a double-blind manner by the biochemical laboratory and the clinic (Jianheng Diabetic Hospital, Beijing, China). Urine D-ribose and D-glucose were measured as described previously (Su et al., 2013). A 1.0 ml urine sample (thawed at 4 °C) was pipetted into 1.5 ml Eppendorf tube and centrifuged (12,000 rpm, 4 °C, and 30 min). Serum proteins were then precipitated by addition of three-fold acetonitrile and were centrifuged (12,000 rpm, 4 °C, and 10 min). A 0.4 ml aliquot of the supernatant was mixed with 0.6 ml 4-(3-methyl-5-oxo-2-pyrazolin-1-yl) benzoic acid (MOPBA, final concentration 150 mM, in 250 mM NaOH in 50% methanol-water solution). Samples were vortexed vigorously for 30 s before centrifugation (12,000 rpm, 4 °C, and 10 min) and then heated in a 70 °C water bath for 90 min; this was followed by additional centrifugation (12,000 rpm, 4 °C, and 10 min). The mixture was acidified by addition of 150 μl of aqueous 2 M HCl solution to precipitate the excess MOPBA. The mixture was vigorously vortexed and centrifuged (12,000 rpm, 4 °C, and 10 min) and then filtered (0.22 μm). Twenty microliters of the solution was then subjected to high-performance liquid chromatography (HPLC).

The HPLC system (LC-20A, Shimadzu, Japan) was equipped with an ultraviolet detector. The MOPBA-sugar derivative was collected from the C18 column with a binary mobile phase gradient. Mobile phase A was 10 mM of sodium 1-hexanesulfonate; the pH was stabilized at 2.5 by phosphoric acid. Mobile phase B was 50% acetonitrile solution. The elution conditions were 38%–60% B for 15 min, 100% B for 5 min, and 38% B for 5 min. The flow rate was 1 ml/min, and the column temperature was 40 °C. The procedure for D-ribose analysis was identical to the procedure for detecting D-glucose, except in the latter phase, in which the elution conditions were 42%–60% B for 15 min, 100% B for 5 min, and 42% B for 5 min, and 2 μl of the solution was injected into the analytical column. The reference concentrations of D-ribose and D-glucose were determined according to the standard curve.

2.5. In Vitro Studies

Blood samples were obtained from healthy volunteers from 20 to 40 years of age. Whole blood was treated with EDTA anticoagulant and incubated with 0.2 mM D-ribose, 7 mM D-ribose or 7 mM D-glucose in a rigorous sterile operation; as in a previous study, the urine D-ribose level was approximately 0.2 mM (Su et al., 2013a). The samples were warmed in a 37 °C water bath for 7 days. To observe the effects of different concentrations of D-ribose and D-glucose on red blood cells, blood films were used, as described in a previous study (Warhurst and Williams, 1996). The blood cell numbers were counted with a haemacytometer (Hamaker, 1958).

D-ribose (0.5 mM) was added to foetal calf serum or human urine at 37 °C, and aliquots were collected and used for measurement of D-ribose at different time intervals (0, 2, 4, 6, 8, 24, 36, 48, and 72 h). Haemoglobin (10 mg/ml) was incubated with different concentrations of D-ribose (0, 1, 20, 50, 100, and 200 mM) for 5 days, and aliquots were collected and used for the detection of HbA1c each day. Haemoglobin (10 mg/ml) was incubated with 0.2 mM D-ribose or 7 mM D-glucose (0, 6, 12, 24, 36, 48, 72, and 96 h), and aliquots were collected and used for detection of HbA1c at each interval. HbA1c was determined with an ELISA kit for human HbA1c. All data were from 3 separate experiments.

2.6. Determination of HbA1c

1) Levels of HbA1c (clinical samples) were measured using the ion-exchange HPLC method, as certified by NGSP (Weykamp et al., 2011; Kashiwagi et al., 2012), with an HbA1c detective system MQ-2000PT, according to the manufacturer's instructions (Medconn Corporation, Shanghai, China).

To verify that the ribosylation of Hb produced HbA1c, haemoglobin (final concentration 10 mg/ml, Sigma, USA) was incubated with 100 mM D-ribose or D-glucose for 3 days, and aliquots were collected for measurements with a Human HbA1c Kit (Catalogue #80099, Crystal Chem, USA).

To determine whether D-ribose could enter RBCs, fresh blood (2 ml) was incubated with D-ribose (0.2 mM or 7 mM) or D-glucose for 7 days and centrifuged to isolate blood cells. The cells were treated with lysis buffer, and HbA1c was determined according to the manufacturer's instructions.

2) Mouse and rat HbA1c levels were determined with a Mouse HbA1c Kit (Catalogue #80310, Crystal Chem, USA) and Rat HbA1c kit (Catalogue #80300, Crystal Chem, USA), according to the manufacturer's instructions.
3) To monitor the kinetics of the ribosylation of Hb, the time course of fructosamine formation was determined with an NBT assay Kit (Huili Biotech, China) during the incubation of Hb with D-ribose. First, 500 μl of human haemoglobin (final concentration 10 mg/ml, Sigma, USA) was dissolved in 500 μl of D-ribose or D-glucose (final concentration 100 mM) at 37 °C for 7 days. Then, 100 μl of pre-warmed NBT reagent (Somani et al., 1989; Xu et al., 2002) was added to the 100 μl mixture, and the absorbance was measured at 530 nm in the 96-well plates for a time interval between 5 min (A1) and 10 min (A2) on a multiscan spectrum (SpectrMax Para4digm, Molecular Devices, USA). The $\Delta A = A2 - A1$ was measured, and the data were expressed as ΔA/min.
4) To investigate the potential contribution of D-ribose to HbA1c formation, different concentrations of D-ribose (0, 1, 20, 50, 100, and 200 mM) were incubated with human haemoglobin (10 mg/ml) (H7379, Sigma, USA) at 37 °C for five days. The levels of HbA1c were detected with an Enzyme-linked Immunosorbent Assay kit (CEA190Hu, Cloud-Clone Corp., China) for human HbA1c each day.

2.7. Analysis of Carboxymethyl-L-lysine in HbA1c by LC-MS/MS

Human haemoglobin (final concentration 10 mg/ml) was incubated with D-ribose (1 M) for four days, and aliquots (containing 10 μg protein) were collected daily and used for analysis by 15% SDS-PAGE. The bands were excised from the polyacrylamide gel, washed twice with double-distilled water, and destained with 40% acetonitrile/50 mM NH_4HCO_3 for CBB staining. The gel pieces were dehydrated with 100% acetonitrile and dried for 5 min with a SpeedVac. Disulfide bonds were reduced with DTT (10 mM, 56 °C, 45 min), and free sulfhydryl groups were alkylated with iodoacetamide (55 mM, 25 °C, 60 min in the dark). Gel pieces were washed with 50 mM NH_4HCO_3, then 50% acetonitrile/50 mM NH_4HCO_3, and dehydrated with 100% acetonitrile. After being dried with a SpeedVac, the gel was rehydrated with 100 ng/μl chymotrypsin (50 mM NH_4HCO_3, pH = 8.3) on ice for 30 min, and the digestion was carried out at 37 °C for 60 min and then quenched with

1.0% formaldehyde. The chymotryptic peptides were extracted twice with 60% acetonitrile containing 0.1% formaldehyde, and then the combined digest solution was concentrated to 10 μl under vacuum.

All analyses were performed on a nano-LC-LTQ-Orbitrap XL mass spectrometer at a resolution of 60,000 (Thermo, San Jose, CA) (Lopez-Clavijo et al., 2014; Tessier et al., 2016). For nano-LC-LTQ-Orbitrap XL MS/MS, chymotrypsin-digested peptides were separated with a C18 reverse phase column (filled with 3-μm ReproSil-Pur C18-AQ from Dr. Maisch GmbH, Ammerbuch, Germany) and loaded through a C18 reverse phase column (filled with 5-μm ReproSil-Pur C18-AQ from Dr. Maisch GmbH) into the LTQ-Orbitrap MS/MS system. Data were analysed with Proteome Discoverer Software (version 1.4.0.288, Thermo Fischer Scientific). The second MS spectra were searched in the human database by using the SEQUEST search engine. The mass accuracy was set at 20 ppm for MS mode and at 0.6 Da for MS/MS mode, and two missed chymotryptic cleavage sites were allowed in the search. Carboxymethyl-L-lysine (CML) and the oxidation of methionine and proline were set as variable modifications. Cam of cysteine was set as a fixed modification. The matching of the searched peptide and MS spectra was filtered by Percolator calculation. The raw mass spectrometry data are available online (http://pan.baidu.com/s/1kVoJV4V).

2.8. Animals and Treatments

Male C57BL/6J mice (8 weeks) were obtained from Vital River Laboratory Animal Technology Co. Ltd. (China). After 1 week of acclimatization to the cages, the mice were randomly divided into three groups (12 mice per group) and received intraperitoneal D-ribose injections each day for 7 days. The treatment doses were 4 g/kg (D-ribose), 4.8 g/kg (D-glucose), and 0.9% saline as control (Han et al., 2011).

Male Sprague-Dawley (SD) rats (150–200 g) were obtained from Vital River Laboratory Animal Technology Co. Ltd. (China). A type 1 diabetic animal model was prepared as previously described (Leehey et al., 2008; Erdal et al., 2012) through a single intraperitoneal injection of STZ (65 mg/kg body weight, Sigma, USA). Control rats matched for age and body weight received an equal volume of the vehicle. After 7 days, diabetic rats were assigned to three groups with different intraperitoneal injections (once daily, for 7 days) of D-ribose at a dose of 4 g/kg (STZ + R), D-glucose at a dose of 4.8 g/kg (STZ + G), or 0.9% saline (STZ). There were 12 rats in each group (Han et al., 2011). Age- and weight-matched SD rats without the treatments were used as controls. Animals were sacrificed after 2 weeks of treatment. All rats were maintained in animal facilities under pathogen-free conditions.

Male ZDF rats (ZDF/Gmi-fa/fa) and LEAN control rats (ZDF/Gmi-fa/+) were obtained from Vital River Laboratory Animal Technology Co. Ltd. (China) at an age of 10 weeks. These rats spent a week in their new cages to acclimate. Animals were sacrificed at the age of 18 weeks. LEAN rats were divided into three groups: rats fed a normal diet (L-N), rats fed a normal diet but injected (i.p.) with 65 mg/kg STZ (L-STZ) one week before sacrificed, and rats fed a Purina 5008 diet (L-P). ZDF rats were maintained on a Purina 5008 diet.

Male ZDF rats (ZDF/Gmi-fa/fa) and LEAN control rats (ZDF/Gmi-fa/+) were obtained from Vital River Laboratory Animal Technology Co. Ltd. (China) at an age of 10 weeks and were maintained on a Purina 5008 diet. The rats were divided into four groups: a group of ZDF rats gavaged with benfotiamine for 4 months (Fraser et al., 2012) (ZDF-Ben, n = 13), a group of ZDF-Ben with benfotiamine withdrawn at the end of the 8th week (Withdrawal, n = 14), a group of ZDF rats gavaged with carboxymethylcellulose sodium (ZDF-CMC, n = 14), and the L-P group (n = 15). All rats were maintained in animal facilities under pathogen-free conditions and were sacrificed at the end of the 4th month.

All the mice and rats were maintained in animal facilities under pathogen-free conditions. All animal experiments were conducted in accordance with the National Institutes of Health Guide for the Care and Use of Laboratory Animals and were approved by the Biological Research Ethics Committee of the Institute of Biophysics, Chinese Academy of Sciences (Permit Number: SYXK2013-33).

2.9. Sample Collection

When mice and rats were sacrificed, their blood was placed at room temperature for 30 min, then centrifuged (3000*g*, 20 min, 4 °C) (Weng et al., 2007). The serum was aspirated and stored at −80 °C until analysis. At the same time, the liver was quickly dissected out and then either immediately homogenized in RIPA Lysis Buffer (Beyotime, China) and centrifuged to yield supernatants for western blotting, or fixed in 4% paraformaldehyde for immunohistochemical experiments.

2.10. Blood Physiochemical Assays

Fasting Blood Glucose (FBG) was measured using the glucose oxidase method, with an automatic biochemical analyser D280 (Sinnowa Corporation, Jiangsu, China). Blood insulin, C-peptide, insulin autoantibody (IAA) and glucagon were determined with a Rat C-Peptide RIA Kit (RCP-21K, LINCO Research, USA), Rat Insulin RIA Kit (RI-13K, LINCO Research, USA), Insulin Autoantibody (IAA) RIA Kit (KR6790, KRONUS, USA), and Glucagon RIA Kit (GL-32K, LINCO Research, USA), respectively, with a DFM-96 radioimmune γ counter (Zhongcheng Corporation, Hefei, China).

2.11. Western Blotting and Enzyme Activity Assay

The concentrations of tissue protein extracts were quantified with a BCA Protein Assay Kit (Pierce, USA). Equivalent amounts of tissue protein extracts (50 μg) were resolved on 12% SDS-PAGE gels and transferred to PVDF membranes. Membranes were then incubated with anti-transketolase polyclonal antibodies (A91959, 1:2000, Sigma, USA) or anti-β-actin monoclonal antibodies (A1978, 1:10000, Sigma, USA) overnight at 4 °C. Each membrane was washed three times with PBS with 0.1% (v/v) Tween-20 (PBST, pH = 7.4), and then incubated with horseradish peroxidase-conjugated anti-mouse IgG at 37 °C for 1 h. The membranes were washed three more times with PBST, and then immunoreactive bands were visualized using enhanced chemiluminescence detection reagents (Applygen, China). The protein bands were visualized through exposure of the membranes to Kodak X-ray film and quantified with Quantity One 1D analysis software 4.5.2 (Bio-Rad, USA). The results were from at least three independent experiments.

The TK activity in the liver was assayed by using a Rat ELISA kit (Invitrogen, USA) according to the manufacturer's instructions. The results were from at least three independent experiments.

2.12. RNA Extraction and Real-time PCR

Total RNA was extracted from the tissues with an RNeasy Micro Kit (Qiagen, Germany) according to the manufacturer's instructions. First-strand cDNA synthesis was performed with M-MLV Reverse Transcriptase (Promega, USA). The following primers were used for PCR: TK (forward: 5′-TTCGGTCGGTCCCTATGT-3′, reverse: 5′-GGAAATCCTCGTTGTTGCTAT-3′) and β-actin (forward: 5′-CACCCGCGAGTACAACCTTC-3′, reverse: 5′-CCCATACCCACCATCACACC-3′). PCR was conducted using normalized amounts of template. The number of PCR cycles performed varied from 24 to 30 depending on the individual gene. An annealing temperature of 56 °C was used for the TK and β-actin primers. For real-time PCR, the resultant cDNA was diluted 1:20. The PCR reactions were performed with a TransStart Green qPCR SuperMix UDG kit (Transgen, China) on an MJ Research Chromo4 detector (Bio-Rad) by using a SYBR green fluorescence quantification system. The relative expression level was calculated by the $2^{-\Delta\Delta Ct}$ method. The means ± s.d. are from three independent replicates.

2.13. Immunofluorescence Staining

Rat livers were immersed in 4% paraformaldehyde for 48 h immediately after dissection. After fixation, the liver tissues were embedded in paraffin blocks. Five micrometre thick sections were processed for immunofluorescent staining. After deparafinization, hydration, and immunoreactivity enhancement, the sections were incubated in 10% normal goat serum in PBS at room temperature for 30 min and probed overnight at 4 °C with anti-transketolase polyclonal antibody diluted in TBST buffer. Bound antibodies were visualized with Alexa 488-conjugated anti-mouse IgG (Invitrogen, USA), and cell nuclei were stained with the DNA-specific fluorescent reagent Hoechst 33258. Immunolabelled tissues were observed under an AEC microscope (Nikon Optical, Japan). The results were from at least three independent experiments.

2.14. Statistical Analysis

The significances between two groups were calculated with two-sided unpaired Student *t*-tests. The demographic variables of more than two groups were assessed using one-way analysis of variance (ANOVA) for continuous variables or a χ^2 analysis for categorical variables. Correlations between urine D-ribose and HbA1c, as well as between urine D-glucose and HbA1c, were assessed using partial correlation methods. Linear regression (stepwise method) was conducted to assess the influence of D-ribose and D-glucose on HbA1c. P values of < 0.05 were considered significant. All statistical analyses were performed using SPSS 17.0 (International Business Machines Corporation, USA).

3. Results

3.1. Glycation of Haemoglobin in the Presence of D-Ribose

Clinically, elevated HbA1c is used as a criterion to support the diagnosis of diabetes. The human HbA1c Kit (Dooley et al., 2016; ElGendy and Abbas, 2014; Mul et al., 2012), which uses the specific fructosyl valine oxidase (FVO) enzyme to cleave N-terminal valines (Liu et al., 2008), was used to test whether the ribosylation of Hb produces HbA1c. As shown in Fig. 1a, D-ribose reacted with the N-terminal valinyl residues of Hb, thus producing significantly higher HbA1c levels ($P < 0.001$) than D-glucose after three days of incubation with 0.1 M D-ribose or 0.1 M D-glucose. This result demonstrated that both D-ribose and D-glucose glycate Hb and produce HbA1c.

To clarify how quickly D-ribose reacts with haemoglobin, an NBT assay was performed to determine the formation of fructosamine during the incubation of human haemoglobin with D-ribose at 37 °C. As shown in Fig. 1b, fructosamine significantly increased with time in the D-ribose group, compared with the D-glucose group, especially during the initial two days. Using Tsou's method (Tsou, 1962), we found that the first-order rate constant of fructosamine formation in the D-ribose group ($98.72 \times 10^{-7} \cdot s^{-1}$) was approximately 60 times greater than in the D-glucose group ($1.65 \times 10^{-7} \cdot s^{-1}$; Fig. 1c). In other words, under the experimental conditions, D-ribose glycates haemoglobin more rapidly than D-glucose in vitro.

Because Hb exists in red blood cells (RBCs), whether D-ribose enters the cells needs to be demonstrated. As shown in Fig. 1d, the HbA1c levels in blood cells were significantly higher ($P < 0.05$, $n = 15$) in the D-ribose group as well as in the D-glucose group, compared with the control group. A significant increase ($P < 0.05$, $n = 15$) in HbA1c was

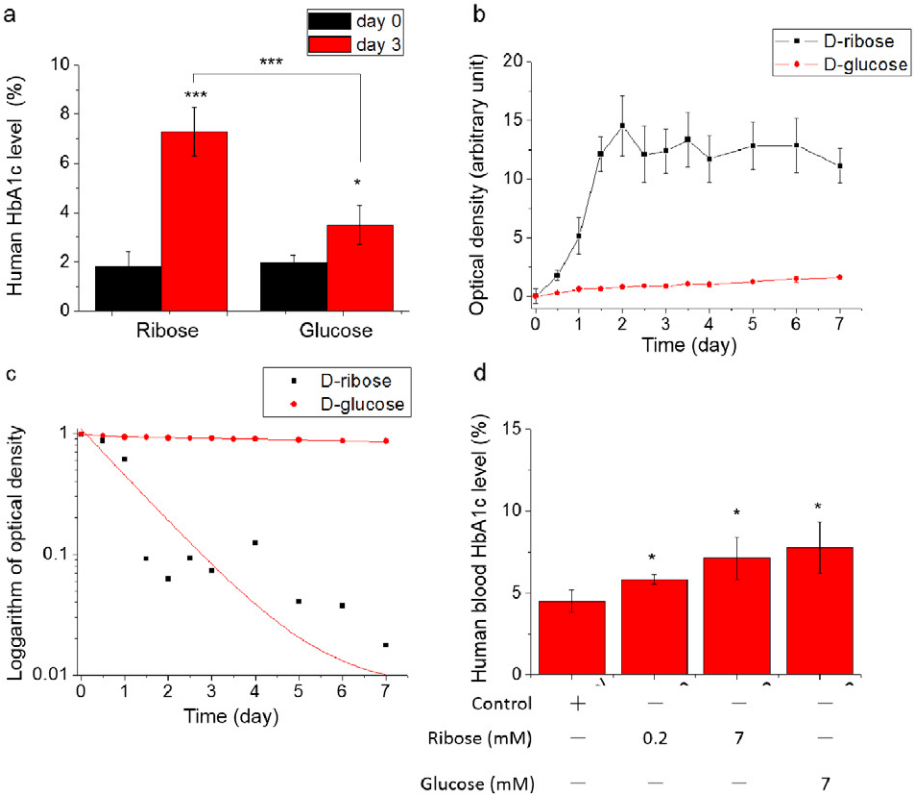

Fig. 1. Glycation of haemoglobin in the presence of D-ribose in vitro and in vivo. (a) The formation of HbA1c was determined during the incubation of human haemoglobin (60 mg/ml) with 0.1 M D-ribose or 0.1 M D-glucose for 3 days. (b) The formation of fructosamine was determined during the incubation of human haemoglobin (60 mg/ml) with 0.1 M D-ribose and 0.1 M D-glucose. (c) The first-order rate constant of fructosamine formation was analysed by Tsou's method (Tsou, 1962). The level of HbA1c was determined after incubation of haemoglobin (Liu et al., 2008) with D-ribose or D-glucose. (d) Human whole blood was supplemented with 0.2 mM D-ribose, 7 mM D-ribose and 7 mM D-glucose at 37 °C for 7 days. The levels of HbA1c were determined with a human HbA1c kit ($n = 15$). Data are shown as the mean ± s.d.; *, $P < 0.05$; ***, $P < 0.001$.

observed in the presence of 200 μM D-ribose. During incubation, the cells were maintained almost intact (Fig. S1a–d), and the cell numbers decreased slightly, by 5.05%, 9.45% and 6.59% for the 200 μM D-ribose group, 7 mM D-ribose group and 7 mM D-glucose group, respectively (Supplementary Table S1). These results showed that D-ribose can enter RBCs and produce HbA1c.

To clarify which amino acid residue is ribosylated in HbA1c, we incubated Hb with D-ribose, collected aliquots at different time intervals and performed SDS-PAGE analysis (Fig. S2a). The apparent molecular masses of HbA1c increased in the presence of D-ribose. The protein bands were digested with 100 ng/μl chymotrypsin, and the fragments were analysed with a mass spectrometer. We found 10 lysinyl residues to be chemically modified (Fig. S2b). As shown in Fig. S2c, one of the ribosylated Hb polypeptides was 58 Da heavier than the control (Fig. S2d). The difference in molecular mass between carboxymethyllysine (CML, 205 Da) and lysine (147 Da) is 58 Da (Tessier et al., 2016). These data indicated the yield of CML resulting from ribosylation.

To investigate the kinetic changes in HbA1c levels in the presence of D-ribose, we incubated human Hb with different concentrations of D-ribose for different time intervals (Fig. S3a). The levels of HbA1c and D-ribose were linearly correlated during the initial stage of the reaction (Fig. S3b). To mimic in vivo conditions, 0.2 mM D-ribose and 7 mM D-glucose were added to human Hb (10 mg/ml), and aliquots were collected at different intervals for measurement (Fig. S3c). The initial amounts of HbA1c were higher in the presence of D-ribose than of D-glucose.

3.2. Administration of D-ribose Leads to the Elevation of HbA1c

To investigate whether D-ribose levels are correlated with HbA1c levels, we treated wildtype C57BL/6 (C57) mice ($n = 12$) with D-ribose by intraperitoneal injection for a period of 7 days. The D-ribose-treated mice, compared with those in the other groups, showed no significant difference ($P > 0.05$) in their body weights (Fig. S4a). However, their blood D-glucose concentrations were significantly lower than those in the positive control group ($P > 0.05$; Fig. S4b). As shown in Fig. S4c, HbA1c was significantly increased ($P < 0.05$) by the injection of D-ribose compared with the levels after D-glucose injection and the control levels. A marked increase in blood D-ribose was observed ($P < 0.001$) in the D-ribose-injected group but not in the D-glucose- or saline-injected groups (Fig. S4d). This result indicates that HbA1c is elevated in wildtype C57 mice as a consequence of D-ribose administration.

Because the relationship of D-ribose with HbA1c was revealed in wildtype C57 mice, we sought to investigate whether D-ribose also affects HbA1c in diabetic Sprague-Dawley (SD) rat models. To determine whether ribosylation is reactive in the glycation of haemoglobin, we injected high doses of streptozotocin (STZ, 65 mg/kg body weight) to damage the islet β-cells in SD rats and thereby developed an STZ model (Erdal et al., 2012). These rats were intraperitoneally injected with D-ribose (once daily) for one week. The levels of HbA1c showed an increase but not significant in the STZ model. This may be due to the 14-day procedure but not so long as the life span of rat Hb is 68 days (Van Putten, 1958). However, HbA1c was significantly ($P < 0.05$) increased in STZ rats injected with D-ribose (STZ + R) compared with rats injected with D-glucose (STZ + G) or saline (STZ), or rats without STZ in the control group ($n = 12$ each group; Fig. 2a). The body weights of the rats in all treated groups decreased compared with those in the control group ($P < 0.05$), but no significant differences among the treated groups ($P > 0.05$; Fig. S5a).

To demonstrate whether the increase in HbA1c resulted from D-ribose, the blood D-ribose levels were measured. The blood D-ribose of STZ + R was markedly elevated, but no significant increase in the D-ribose levels of STZ + G was observed ($n = 12$, $P > 0.05$; Fig. 2c), thus indicating that D-glucose had a weak effect on D-ribose level. The rats treated with saline did not show a significant ($P > 0.05$) increase in blood D-ribose. These data suggested that the elevation of HbA1c in STZ rats was a result of the administration of D-ribose rather than D-glucose.

To investigate the metabolism of D-ribose after injection, we measured urine D-ribose in the rats (Fig. 2b). On one hand, a marked increase in urine D-ribose was observed in STZ + R, in contrast with the other groups ($n = 12$, $P < 0.001$). On the other hand, the injection of D-ribose did not increase the concentration of either blood or urine D-glucose ($P > 0.05$; Fig. 2d, Fig. S5b). The STZ rats administered D-ribose, D-glucose and saline showed low levels of blood insulin (Fig. S5c). Together, our results indicated that the increase in HbA1c was mainly caused by D-ribose.

3.3. HbA1c Levels in ZDF Rats are Associated With D-Ribose Levels

To further demonstrate the relationship between HbA1c and D-ribose in vivo, we used Zucker diabetic fatty (ZDF/Gmi-fa/fa) rats fed a Purina 5008 diet (ZDF rat), which is an accepted T2DM animal model (Kawaguchi et al., 1999). As described by Pold et al. (2005), age-matched LEAN (ZDF/Gmi-fa/+) rats were used as controls for ZDF rats (Fig. S6a). LEAN rats were divided into three groups: rats fed with a normal diet (L-N), rats fed with a normal diet but injected (i.p.) with 65 mg/kg STZ (L-STZ), and rats fed with a Purina 5008 diet (L-P). The body weights of both ZDF rats ($n = 11$, $P < 0.001$) and age-matched L-P rats ($n = 12$, $P < 0.05$) increased after rearing for 4 weeks. However, the weights of the ZDF rats increased to a significantly greater extent than all other groups (Fig. S6b). The levels of urine D-glucose in the L-STZ ($n = 10$) and ZDF groups were significantly higher than those in the L-N ($n = 12$) and L-P groups, although significant differences ($P > 0.05$) were not observed between the L-STZ and ZDF groups (Fig. S6c). The levels of blood insulin were decreased in L-STZ rats. The insulin autoantibody level (IAA) was significantly increased ($P < 0.01$) in the L-STZ rats compared with the L-N rats. The ZDF rats had significantly higher levels of insulin, C-peptide, and IAA, thus indicating insulin resistance (Fig. S6d, e, f). Notably, both urine D-ribose and D-glucose levels of ZDF rats were significantly elevated ($P < 0.001$) after feeding a Purina 5008 diet for one week (above the pre-treatment levels of ZDF-N; Fig. S6g, h).

Under the experimental conditions, the ZDF rats had higher levels of HbA1c than did age-matched L-P, L-STZ, and L-N rats (Fig. 3d). Both urine and blood D-ribose levels were significantly increased ($P < 0.001$) in ZDF rats but not in the other three groups (Fig. 3e, f). Blood D-glucose levels increased ($P < 0.001$) in both the L-STZ (19.80 ± 1.58 mM) and ZDF groups (20.48 ± 2.79 mM), though there were no significant differences ($P > 0.05$) between the two groups (Fig. 3g). These results revealed that the higher level of HbA1c in the ZDF rats was dependent on D-ribose.

3.4. Inactivation of Transketolase in ZDF Rats

Transketolase (TK) is the most active enzyme involved in the non-oxidative branch of the pentose phosphate pathway (Matsushika et al., 2012) and generates the ribose-5-P molecules necessary for aerobic or anaerobic metabolism (Su and He, 2014). To clarify the mechanisms leading to high levels of D-ribose, we investigated the TK expression and enzymatic activity in ZDF rats (Fig. 3a). The protein level and enzymatic activity of TK ($P < 0.001$) were markedly decreased in the livers of ZDF rats (Fig. 3b, c). In contrast, neither the L-P group nor the L-STZ group showed significant decreases ($P > 0.05$) in TK level or activity. These data suggested that ZDF rats modelling T2DM have a low ability to metabolize D-ribose, owing to the inactivation of TK.

3.5. Benfotiamine Impedes Increases in HbA1c and D-Ribose Through TK Activation

To demonstrate that high levels of D-ribose in the blood and urine resulted from decreased TK levels, ZDF rats were administered

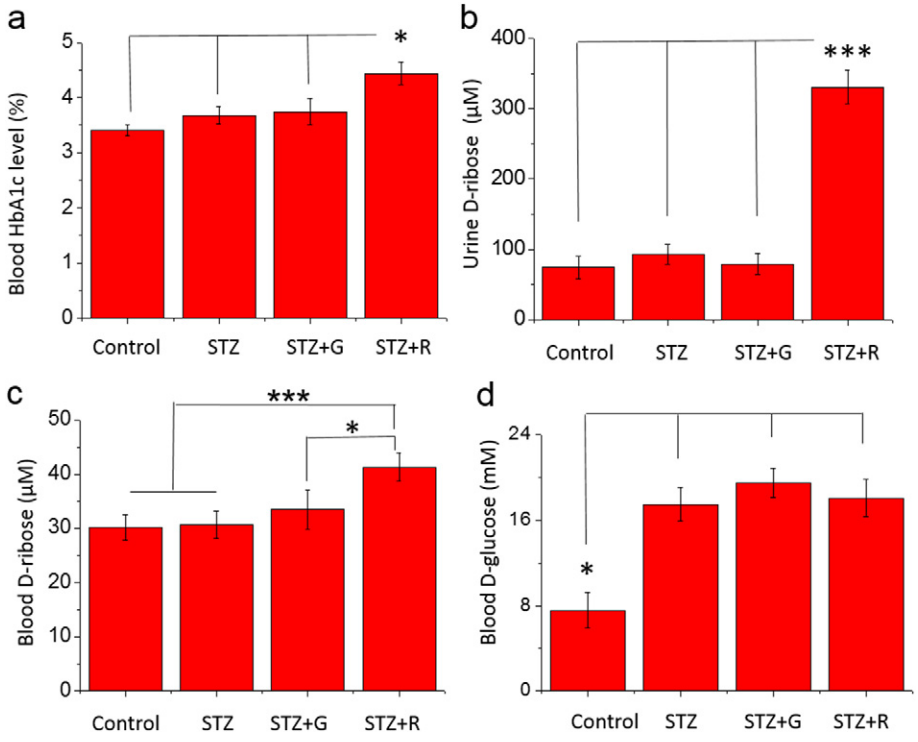

Fig. 2. Accumulation of HbA1c and D-ribose in STZ rats after injection of D-ribose. (a) STZ rats were treated with 65 mg/kg STZ (1 injection, i.p.) and reared for 7 days. HbA1c was measured after STZ rats were injected with D-ribose (4 g/kg) or D-glucose (4.8 g/kg) (once daily) for another 7 days. (b, c and d) Urine D-ribose (b), blood D-ribose (c) and blood D-glucose (d) were detected (n = 12). STZ, STZ rats injected (i.p.) with saline; STZ + R, STZ rats injected (i.p.) with D-ribose; STZ + G, STZ rats injected (i.p.) with D-glucose. All values are expressed as the mean ± s.d.; *, $P < 0.05$; ***, $P < 0.001$.

benfotiamine, an activator of TK (Hammes et al., 2003). The rats were divided into four groups: a group of ZDF rats gavaged with benfotiamine for 4 months (Fraser et al., 2012) (ZDF-Ben, n = 13), a group of ZDF-Ben with benfotiamine withdrawn at the end of the 8th week (Withdrawal, n = 14), a group of ZDF rats gavaged with carboxymethylcellulose sodium (ZDF-CMC, n = 14), and the L-P group (n = 15) as described above. After one month, the ZDF-Ben rats showed a marked decrease in urine D-ribose, as compared with the ZDF-CMC group, and a similar D-ribose level to that of the L-P group (Fig. 4a). Both the blood D-ribose and HbA1c levels of the ZDF-Ben rats decreased to a normal level, as compared with the controls after a 4-month treatment with benfotiamine. However, when the drug was withdrawn at the beginning of the third month, the levels of blood D-ribose and HbA1c rebounded to pre-treatment levels (Fig. 4b, c). This result indicated that the inactivation of TK contributes to the elevation of D-ribose.

To confirm that the activation of TK resulted in a decrease in HbA1c induced by D-ribose, we further investigated whether TK was rescued by benfotiamine. We found that ZDF-CMC rats had significantly lower ($P < 0.001$) levels of TK (both mRNA and protein) than did L-P rats (Fig. 5a–d). ZDF-Ben rats, compared with ZDF-CMC rats, showed significant increases in TK levels of both mRNA and protein ($P < 0.001$) (Fig. 5a–d). However, TK decreased to the pre-treatment level after benfotiamine was withdrawn. Higher levels of TK expression were observed in liver sections of rats from the L-P and ZDF-Ben groups by immunofluorescence staining, as compared with the ZDF-CMC and Withdrawal groups (Fig. 5e, f, Fig. S7). Therefore, benfotiamine activates TK in the livers of ZDF rats.

To determine whether benfotiamine affects insulin metabolism, after ZDF rats were reared for 4 months, the levels of D-glucose, insulin, C-peptide, IAA, and glucagon in the blood and the body weights were measured (Fig. S8a–f). All levels were significantly higher ($P < 0.001$) in the ZDF-Ben, Withdrawal, and ZDF-CMC groups than in the L-P group. However, the differences in these levels among the ZDF-Ben, Withdrawal, and ZDF-CMC groups were not significant ($P > 0.05$). In other words, benfotiamine did not markedly affect the metabolism of D-glucose, insulin, or glucagon.

3.6. Correlation of Urine D-Ribose and HbA1c Levels in Patients With T2DM

To investigate whether D-ribose is associated with T2DM, we performed a cross-section clinical trial. The participants with HbA1c levels of 5.49 ± 0.30%, 6.93 ± 0.29%, and 9.20 ± 1.05% were divided into the control group, group 1 and group 2, respectively. As shown in Fig. 6, concentrations of urine D-ribose were markedly ($P < 0.05$) higher in group 1 than in the control group. The patients in group 2 had significantly ($P < 0.001$) higher urine D-ribose levels than did both the control group and group 1 (Fig. 6a). Compared with the levels in the control group, the levels of urine D-glucose were significantly elevated in both diabetic group 1 ($P < 0.01$) and group 2 ($P < 0.001$; Fig. 6b). Demographic characteristics of the participants are shown in Table 1.

To assess the association of urine D-ribose with T2DM, a partial correlation analysis was used to analyse the relation between urine D-ribose and HbA1c. Under these conditions (controlling for age, sex, and duration of diabetes), HbA1c levels were correlated not only with urine D-glucose ($r = 0.457$) but also with urine D-ribose ($r = 0.507$). Moreover, the correlation coefficient for urine D-ribose with HbA1c was higher than that for urine D-glucose with HbA1c. As shown in Table 2, urine D-ribose was positively correlated with FBG ($r = 0.370$) and urine D-glucose ($r = 0.285$).

To examine the direction and strength of the association between urine D-ribose and HbA1c, linear regression analysis was applied. The scatter diagrams organized by diabetic patients with different HbA1c levels (Fig. 6c, d), indicated a significant association between urine D-ribose and urine D-glucose levels in the control group ($r^2 = 0.556$, $P < 0.001$, $n = 41$) and group 1 ($r^2 = 0.214$, $P < 0.001$, $n = 38$). However, no similar association was observed in group 2 ($r^2 = 0.002$, $P =$

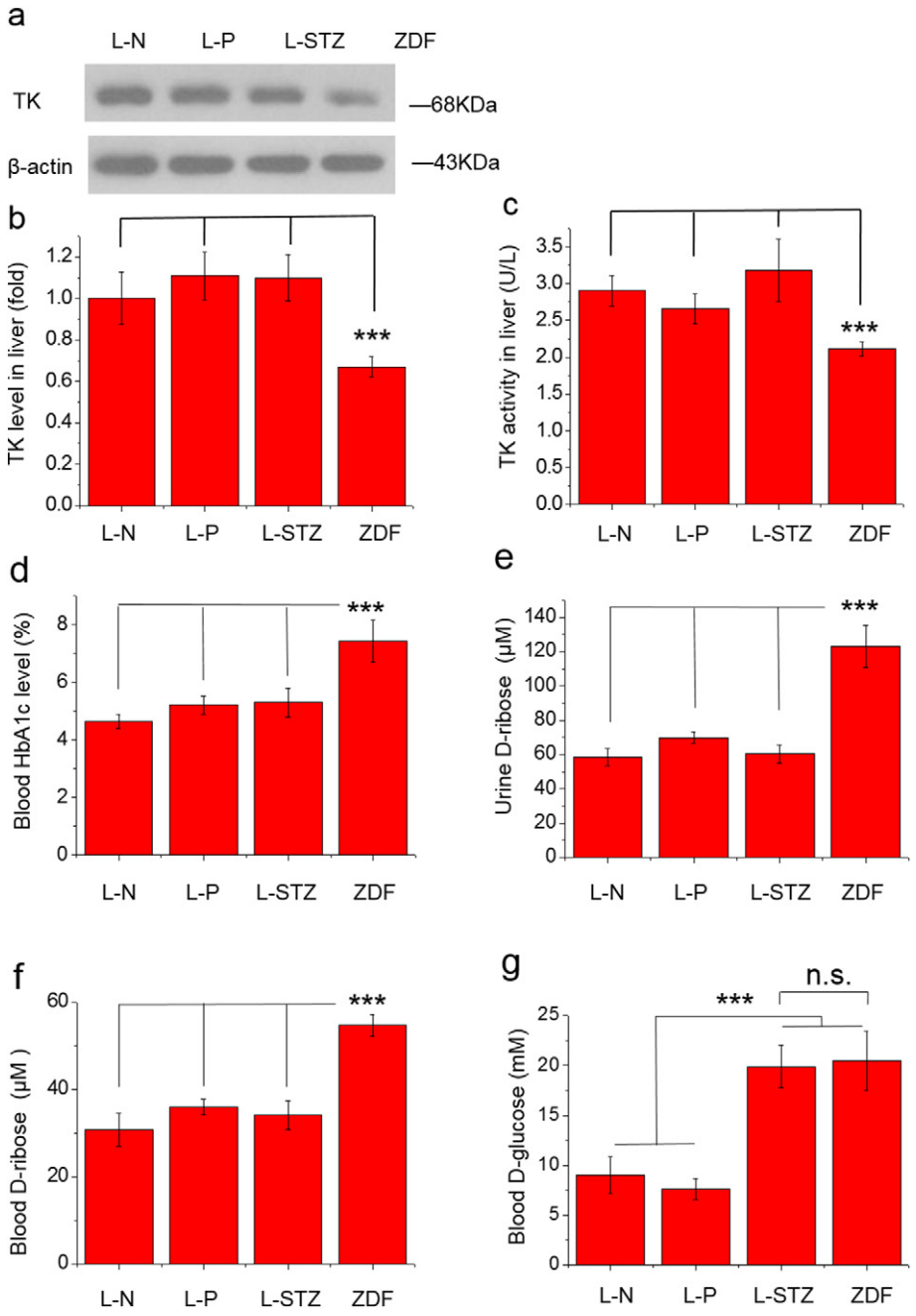

Fig. 3. ZDF rats lack transketolase in their livers. (a) A decrease in TK in the livers of ZDF rats was detected by western blotting using polyclonal anti-TK antibody. β-actin levels were used as loading controls. (b) Quantification by western blotting showed statistically significant decreases in TK levels in ZDF rats. (c) Inactivation of TK in ZDF rats was assayed with an ELISA kit. (d, e, f and g) The levels of HbA1c and blood and urine D-ribose in ZDF rats were elevated. HbA1c (d), urine D-ribose (e), blood D-ribose (f) and blood D-glucose (g) of L-N, L-P, L-STZ and ZDF rats were measured. LEAN rats fed a normal diet served as controls (L-N, n = 12), with a Purina 5008 diet (L-P, n = 12), or injected (1 injection, i.p.) with 65 mg/kg STZ (L-STZ, n = 10). ZDF rats (ZDF, n = 11) were fed a Purina 5008 diet. The results were from at least three independent experiments. All values are expressed as the mean ± s.d.; ***, $P < 0.001$; n.s., not significant.

0.784, n = 44; Fig. 6e). The elevation in both urine D-ribose and D-glucose levels in group 1 and group 2 revealed that D-ribose may also play a role in the contribution of HbA1c to the development of T2DM. Notably, we collected urine samples rather than serum samples in our clinic trial because D-ribose reacts with proteins and rapidly decreases in serum (Fig. S9a) but not in urine (Fig. S9b).

4. Discussion

T2DM is a group of carbohydrate metabolism disorders characterized by hyperglycaemia, usually caused by an insufficient response to insulin (Chen et al., 2011; Badawi et al., 2010). It has long been known that there is a direct correlation between blood D-glucose and HbA1c (Abdul-Ghani et al., 2011), both of which are thought to be predictors of diabetic complications (Bittencourt et al., 2014). In contrast, D-ribose has, to date, been overlooked as a potential risk factor in the development of T2DM (Yokoi et al., 2013; Su and He, 2015).

D-ribose may play a role in diabetes. The reasons are as follows: (i) the ribosylation of proteins such as alpha-synuclein, Tau protein, and bovine serum albumin (BSA) (Chen et al., 2009; Chen et al., 2010; Wei et al., 2009) occurs much more rapidly than glycation with D-glucose, as a result of D-ribose glycation; (ii) the formation of AGEs in the reaction of proteins with D-ribose is also much quicker than that with D-glucose; (iii) the cytotoxicity of the ribosylation products is higher than that of the glycated products (Wei et al., 2012a, Wei et al., 2015); (iv) a high level of D-ribose may be one of the important risk factors for

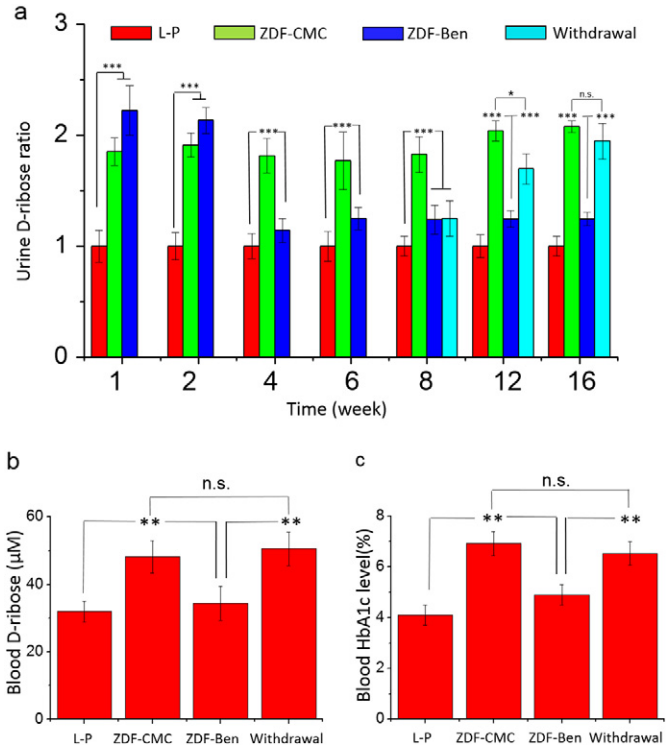

Fig. 4. Benfotiamine decreases the levels of D-ribose and HbA1c in ZDF rats. (a) ZDF rats were administered benfotiamine by gavage (300 mg/kg, once daily) for 4 months, and this was followed by measurements of their urine D-ribose levels at different time intervals (1, 2, 4, 6, 8, 12, and 16 weeks). ZDF rats fed a Purina 5008 diet were gavaged with benfotiamine (ZDF-Ben, n = 13). Benfotiamine was mixed into sodium carboxymethylcellulose (CMC). The other three groups were as follows: LEAN rats fed a Purina 5008 diet (L-P, n = 15), ZDF rats fed a Purina 5008 diet and gavaged with CMC (ZDF-CMC, n = 14), and a ZDF-Ben group withdrawn from benfotiamine at the end of the 8th week (Withdrawal, n = 14). The levels of D-ribose in L-P at each week were normalized to 100%. The levels of urine D-ribose were measured. (b) The levels of blood D-ribose were measured. (c) The levels of HbA1c were measured. All values are expressed as the mean ± s.d.; *, $P < 0.05$; **, $P < 0.01$; ***, $P < 0.001$; n.s., not significant.

the formation of HbA1c in the development of diabetes; and (v) decreasing the concentration of D-ribose with benfotiamine results in a decrease in glycated haemoglobin. Therefore, the role of an increase in D-ribose and the subsequent ribosylation of proteins in the progression of T2DM should not be neglected.

As described previously (Wei et al., 2009), ribosylated proteins are highly toxic to neuroblast cells; the lethal dose of 50% (LD50) is as low as ~6 μM ribosylated BSA. Attention should be paid to the effects of elevated serum D-ribose levels, although the complications resulting from the ribosylation remain to be clarified. The highest level of urine D-ribose observed in T2DM patients was 490 μM. Han et al. have demonstrated that a high level of D-ribose triggered inflammation in the mouse brain, thus leading to cognitive impairment (2011, 2014). High levels of D-ribose also led to the hyperphosphorylation of Tau through the activation of CaMKII (Wei et al., 2015). Long-term (6 months) feeding of wildtype C57 mice not only induced the formation of amyloid β-like deposits but also induced Tau hyperphosphorylation and aggregation, accompanied by cognitive impairments (Wu et al., 2015). In short, ribosylation may be an important risk factor involved in the formation of HbA1c.

Clinically, the measurement of D-ribose from urine has been considered much more precisely than from blood, as urine contains only traces of proteins and other bio-macromolecules (Bair and Krebs, 2010). The contamination possibilities in the D-ribose analysis of urine samples was much less than in blood samples, thus the clinic data through urine D-ribose measurements are convincing. As mentioned above, morning urine samples were collected from T2DM patients (n = 123) by nurses in clinics. It is difficult to obtain accurate data of D-ribose in clinical blood samples collected by nurses on different days because D-ribose is highly reactive with blood proteins, thus resulting in error values out of range, although the method used can precisely determine the concentration of D-ribose. Therefore, it was crucial to determine the concentration immediately after sampling. Determination was performed by using 4-(3-methyl-5-oxo-2-pyrazolin-1-yl) benzoic acid (MOPBA) chromogenic reagent with HPLC methods (Su et al., 2013b). Serum proteins or other unknown biochemical molecules may interfere with the analysis, thus leading to bias and poor reproducibility. However, in the animal experiments, we controlled the conditions, thereby providing reliable blood D-ribose data with low errors. This is to say, a method to determine blood D-ribose in the clinic or at home still needs to be developed.

We believe that patients with diabetes suffer from dysmetabolism involving not only D-glucose but also D-ribose. This viewpoint, that D-ribose plays an important role in the formation of HbA1c, is based on the following observations: (i) chemical modification of HbA1c by D-ribose produces carboxymethyllysines (CMLs), as identified by mass spectrometry (Lopez-Clavijo et al., 2014; Tessier et al., 2016); (ii) elevated levels of D-ribose result in increased ribosylation and the accumulation of advanced glycation end products (AGEs) in SH-SY5Y cells (Wei et al., 2012, Wei et al., 2009); (iii) ZDF rats have high levels of D-ribose in the blood and urine, caused by the low activity of TK; (iv) benfotiamine has been proposed to antagonize diabetes (Babaei-Jadidi et al., 2003, 2005) through the activation of TK, which suppresses D-ribose levels; (v) abnormal increases in urine D-ribose levels have been reported in diabetic patients (Su et al., 2013a, Chen et al., 2016); and (vi) the positive correlation of urine D-ribose with HbA1c in T2DM patients is similar to the pattern for D-glucose.

D-ribose has been detected by high-performance liquid chromatography (HPLC) (Su et al., 2013a) in normal human urine (35.99 ± 5.64 μM male and 33.72 ± 6.29 μM female), in the blood (Cai et al., 2005) and in the cerebrospinal fluid (0.01–0.1 mM) (Seuffer, 1977). The level of ribosylated protein in the blood is still difficult to quantify, because there is no successful method to clarify which glycated protein is induced by D-ribose or D-glucose. D-Ribose reacts with proteins and produces AGEs. The concentration of D-ribose decreases rapidly in the serum, but not in the urine. This difference occurs because D-ribose is present in the blood and is highly reactive in the process of ribosylation before it is excreted in the urine. Furthermore, urine D-ribose levels are positively correlated with HbA1c levels. This finding indicates an inseparable relationship between D-ribose and HbA1c.

Transketolase is a homodimeric enzyme that catalyses the reversible transfer of two carbons from a ketose donor substrate to an aldose acceptor substrate (Zhao and Zhong, 2009; Fullam et al., 2012). TK is the most active enzyme involved in the non-oxidative branch of the pentose phosphate pathway and is responsible for generating the ribose-5-P molecules necessary for nucleic acid synthesis (Schaaffgerstenschlager and Zimmermann, 1993) (Kim et al., 2012). According to Coy et al. (2005), TK levels are markedly decreased in T2DM patients. Thiamine deficiency, as a major risk factor, is widely accepted to be associated with the decrease in TK activity (Brady et al., 1995; Lonsdale, 2015). However, according to the work of Michalak et al. (2013), the decrease in TK activity associated with diabetic neuropathy may be independent of thiamine deficiency. In our study, the elevation of D-ribose was found to be the result of a decrease in TK levels and activity in T2DM. We would like to hypothesize that D-ribose is an important contributors to HbA1c in T2DM patients. Benfotiamine, an activator of TK, may be used to effectively decrease abnormally high levels of D-ribose to decrease HbA1c (Fig. 7).

Benfotiamine counteracts and reverses high D-glucose-induced damage in vascular cells (Tarallo et al., 2012). In the work of Stirban et al. (2006), increased carboxymethyllysine levels in T2DM patients have been prevented by 3-day therapy with benfotiamine. Short-term treatment with benfotiamine counteracts smoking-induced vascular dysfunction (Stirban et al., 2012). According to Gadau et al. (2006),

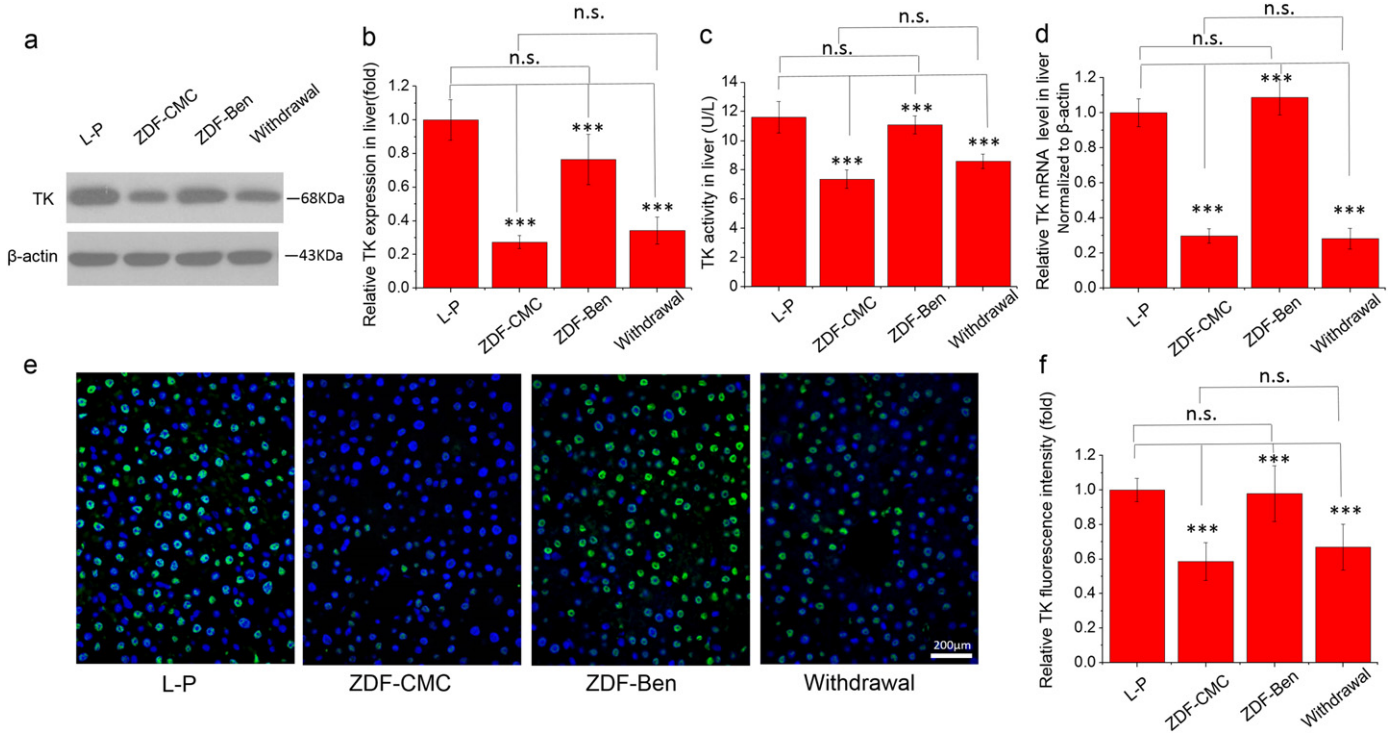

Fig. 5. Benfotiamine rescues the activity of TK in the livers of ZDF rats. (a) Conditions were as in Fig. 4. Levels of TK protein in the livers of ZDF rats were measured by western blotting using polyclonal anti-TK antibody. The β-actin levels were used as loading controls. (b) Quantification of the western blotting results was performed for TK rescued by benfotiamine. (c) The activity of TK was measured with an ELISA kit. (d) The level of TK mRNA in the liver was assayed by real-time PCR. (e) The liver sections were double-labelled for TK with anti-TK (green) and nuclei with Hoechst 33258 (blue). Scale bar, 200 μm. (f) The fluorescent signals of TK in the cells were quantified. The results were from at least three independent experiments. All values are expressed as the mean ± s.d.; ***, $P < 0.001$; n.s., not significant.

benfotiamine is able to aid in the post-ischaemic healing of diabetic animals via the PKB/Akt-mediated potentiation of angiogenesis and the inhibition of apoptosis. HbA1c is a biomarker of glycaemic control that predicts the development of microvascular complications (2011). In this study, D-ribose play an important role in the contribution to HbA1c in ZDF rats. D-ribose levels were closely related to those of

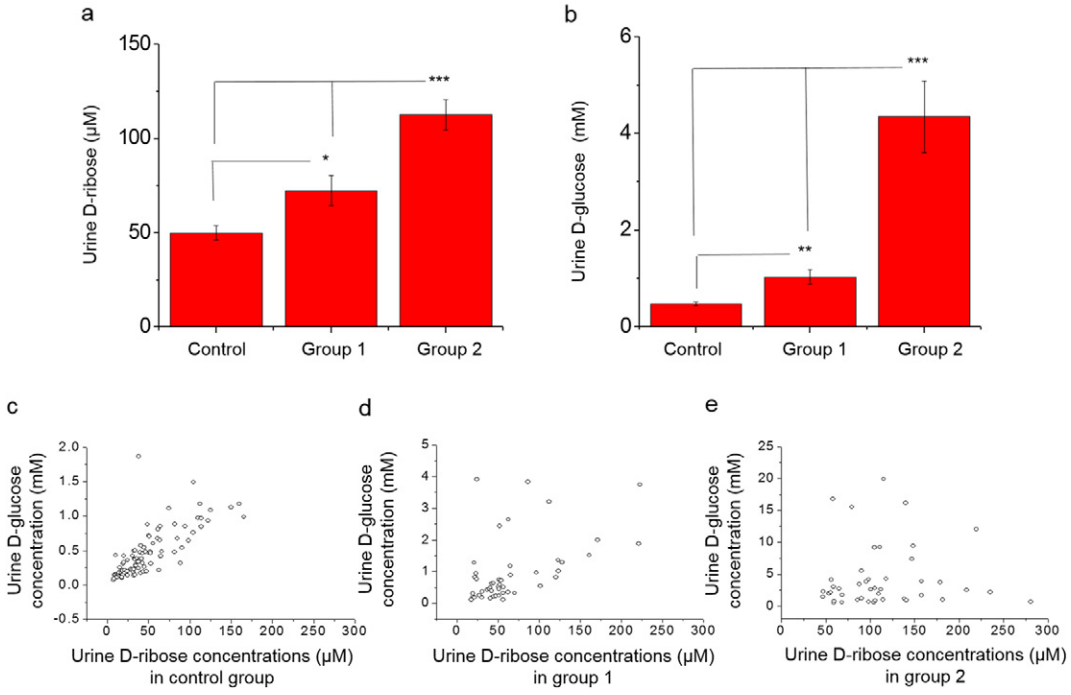

Fig. 6. Concentrations of urine D-ribose and D-glucose in enrolled subjects. (a and b) T2DM patients and age-matched elderly participants without diabetes were enrolled and divided into three groups on the basis of their HbA1c levels: a control group (n = 41, 5.49 ± 0.30%), group 1 (n = 38, 6.93 ± 0.29%), and group 2 (n = 44, 9.20 ± 1.05%). Concentrations of urine D-ribose (a) and D-glucose (b) are plotted in the columns. (c, d and e) the concentrations in the control group (c), group 1 (d) and group 2 (e) are shown in the scatter diagrams. Data were analysed by one-way ANOVA and shown as the mean ± s.e.m.; *, $P < 0.05$; **, $P < 0.01$; ***, $P < 0.001$.

Table 1
Demographic characteristics of participants with different levels of HbA1c.

	Control (n = 41)	Group 1 (n = 38)	Group 2 (n = 44)	P value
Age (years)	61.69 ± 7.22	63.20 ± 6.10	62.63 ± 6.47	0.430
Male (%)	59.21	61.22	50.00	0.301
Diabetes history (years)	–	11.85 ± 7.94	12.05 ± 6.50	0.541
HbA1c (%)	5.49 ± 0.30	6.93 ± 0.29***	9.20 ± 1.05***	<0.001
FBG (mM)	5.64 ± 0.60	6.32 ± 0.75***	8.04 ± 2.05***	<0.001

Data are shown as the mean ± s.d. n, number of individuals. P values were calculated using χ^2 for the categorical variables and ANOVA for the continuous variables.
*** P < 0.001, compared with control group. FBG, fasting blood glucose.

HbA1c in the experiments in vivo and in vitro, thus suggesting that benfotiamine decreases HbA1c through regulating the levels of D-ribose. The relationship between the dysmetabolism of D-ribose and diabetic vascular damage requires further investigation.

In conclusion, the concentration of HbA1c in T2DM patients is positively correlated with urine D-ribose in clinical investigations. ZDF rats, which are commonly used in T2DM studies (Siwy et al., 2012), have high levels of D-ribose and HbA1c in their blood as well as in their urine. Benfotiamine activates TK (Hammes et al., 2003) and decreases blood and urine D-ribose, followed by a decrease in HbA1c in ZDF rats. Thus, D-ribose is one of the important factors in the interpretation of HbA1c, which prompts future studies to explore whether D-ribose could also lead to diabetic complications.

Supplementary data to this article can be found online at https://doi.org/10.1016/j.ebiom.2017.10.001.

Funding Sources

This work was supported by grants from the National Key Research and Development Program of China (2016YFC1305900; 2016YFC1306300), the Beijing Municipal Science and Technology Project (Z161100000217141; Z161100000216137), 973-Project (2012CB911004) and NSFC (31270868, 31670805), The Science and Technology Bureau of Luzhou: Molecular mechanism of diabetic nephropathy (Grant No. 2013-326), and the External Cooperation Program of BIC, CAS (20140909).

Conflicts of Interest

The authors declare no competing financial interests.

Author Contributions

X.X.C. and T.S. performed all the experiments and analysed the data. R.Q.H. designed and supervised this study. Y.G.H. determined D-ribose with HPLC. X.X.C. and T.S. performed animal behavior tests. R.Q.H., Y.W., T.S., X.X.C. and Y.X. wrote the manuscript. X.X.C., T.S., R.Q.H., Y.X., Y.C., J.L. and Y.W. contributed to the revised version.

Table 2
Correlations of urine D-ribose with HbA1c, FBG and urine D-glucose.

	Uric D-ribose		Uric D-glucose	
	r	p	r	p
HbA1c[a]	0.507	<0.001	0.457	<0.001
FBG[a]	0.370	<0.001	0.302	<0.01
Uric D-glucose[a]	0.285	<0.01	–	–

FBG: fasting blood glucose.
[a] The variables were controlled for age, sex, and duration of diabetes. "r" is the correlation coefficient.

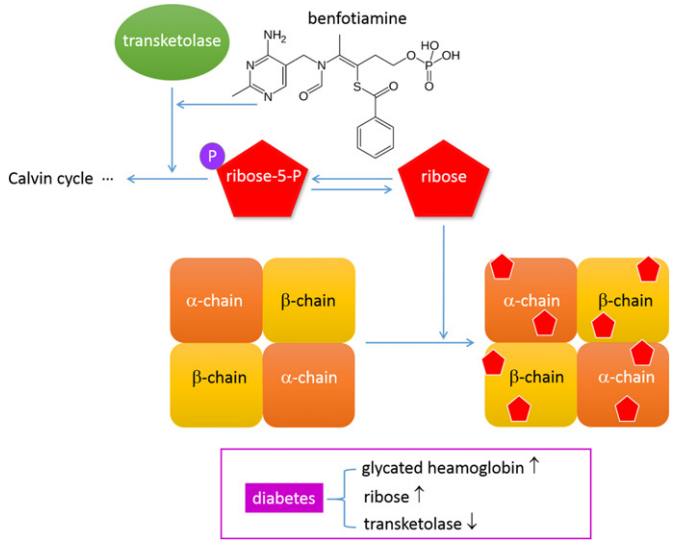

Fig. 7. D-ribose acts as a contributor to glycation of haemoglobin. D-ribose is able to glycate Hb and produces HbA1c. Transketolase (TK) suppresses the yield of D-ribose. HbA1c is downregulated via activation of TK by befotiamine, through decreasing levels of D-ribose.

Acknowledgements

We thank Ling Yan, Jianmei Hang (Jianheng Diabetic Hospital, Beijing) for clinical sample collection, and Visse T.S. Moestrup (CFIN&SDC, Aarhus University, Denmark). We thank Zhensheng Xie and Yinghao Zhang (Institute of Biophysics, CAS) for support in the MS analyses and helpful suggestions. All the funders had no role in study design, data collection, data analysis, interpretation and writing of this manuscript.

References

Abdul-Ghani, M.A., Abdul-Ghani, T., Muller, G., Bergmann, A., Fischer, S., Bornstein, S., Defronzo, R.A., Schwarz, P., 2011. Role of glycated hemoglobin in the prediction of future risk of T2DM. J. Clin. Endocrinol. Metab. 96, 2596–2600.
Babaei-Jadidi, R., Karachalias, N., Ahmed, N., Battah, S., Thornalley, P.J., 2003. Prevention of incipient diabetic nephropathy by high-dose thiamine and benfotiamine. Diabetes 52, 2110–2120.
Babaei-Jadidi, R., Karachalias, N., Ahmed, N., Thornalley, P.J., 2005. Prevention of incipient nephropathy by high dose thiamine and benfotiamine in streptozotocin-induced diabetic rats: effect on markers of oxidative stress. Free Radic. Res. 39, S81.
Badawi, A., Klip, A., Haddad, P., Cole, D.E., Bailo, B.G., El-Sohemy, A., Karmali, M., 2010. Type 2 diabetes mellitus and inflammation: prospects for biomarkers of risk and nutritional intervention. Diabetes Metab. Syndr. Obes. 3, 173–186.
Bair, M.J., Krebs, E.E., 2010. Why is urine drug testing not used more often in practice? Pain Pract. 10, 493–496.
Berg, J.P., 2013. HbA1c as a diagnostic tool in diabetes mellitus. Norsk Epidemiologi 23, 5–8.
Bittencourt, C., Piveta, V.M., Oliveira, C.S., Crispim, F., Meira, D., Saddi-Rosa, P., Giuffrida, F.M., Reis, A.F., 2014. Association of classical risk factors and coronary artery disease in type 2 diabetic patients submitted to coronary angiography. Diabetol. Metab. Syndr. 6, 46.
Brady, J.A., Rock, C.L., Horneffer, M.R., 1995. Thiamin status, diuretic medications, and the management of congestive heart failure. J. Am. Diet. Assoc. 95, 541–544.
Cai, Y., Liu, J., Shi, Y., Liang, L., Mou, S., 2005. Determination of several sugars in serum by high-performance anion-exchange chromatography with pulsed amperometric detection. J. Chromatogr. A 1085, 98–103.
Chen, L., Wei, Y., Wang, X., He, R., 2009. D-Ribosylated tau forms globular aggregates with high cytotoxicity. Cell. Mol. Life Sci. 66, 2559–2571.
Chen, L., Wei, Y., Wang, X., He, R., 2010. Ribosylation rapidly induces alpha-synuclein to form highly cytotoxic molten globules of advanced glycation end products. PLoS One 5, e9052.
Chen, L., Magliano, D.J., Zimmet, P.Z., 2011. The worldwide epidemiology of type 2 diabetes mellitus—present and future perspectives. Nat. Rev. Endocrinol. 8, 228–236.
Chen, L., Cheng, C.Y., Choi, H., Ikram, M.K., Sabanayagam, C., Tan, G.S., Tian, D., Zhang, L., Venkatesan, G., Tai, E.S., Wang, J.J., Mitchell, P., Cheung, C.M., Beuerman, R.W., Zhou, L., Chan, E.C., Wong, T.Y., 2016. Plasma metabonomic profiling of diabetic retinopathy. Diabetes 65, 1099–1108.
Chou, T.H., Wu, P.C., Kuo, J.Z., Lai, C.H., Kuo, C.N., 2009. Relationship of diabetic macular oedema with glycosylated haemoglobin. Eye (Lond) 23, 1360–1363.
Coy, J.F., Dressler, D., Wilde, J., Schubert, P., 2005. Mutations in the transketolase-like gene TKTL1: clinical implications for neurodegenerative diseases, diabetes and cancer. Clin. Lab. 51, 257–273.

Dooley, J., Garcia-Perez, J.E., Sreenivasan, J., Schlenner, S.M., Vangoitsenhoven, R., Papadopoulou, A.S., Tian, L., Schonefeldt, S., Serneels, L., Deroose, C., Staats, K.A., Van Der Schueren, B., De Strooper, B., Mcguinness, O.P., Mathieu, C., Liston, A., 2016. The microRNA-29 family dictates the balance between homeostatic and pathological glucose handling in diabetes and obesity. Diabetes 65, 53–61.

Elgendy, A.A., Abbas, A.M., 2014. Effects of warfarin and L-carnitine on hemostatic function and oxidative stress in streptozotocin-induced diabetic rats. J. Physiol. Biochem. 70, 535–546.

Erdal, N., Gurgul, S., Demirel, C., Yildiz, A., 2012. The effect of insulin therapy on biomechanical deterioration of bone in streptozotocin (STZ)-induced type 1 diabetes mellitus in rats. Diabetes Res. Clin. Pract. 97, 461–467.

Fraser, D.A., Diep, L.M., Hovden, I.A., Nilsen, K.B., Sveen, K.A., Seljeflot, I., Hanssen, K.F., 2012. The effects of long-term oral Benfotiamine supplementation on peripheral nerve function and inflammatory markers in patients with type 1 diabetes a 24-month, double-blind, randomized, placebo-controlled trial. Diabetes Care 35, 1095–1097.

Fullam, E., Pojer, F., Bergfors, T., Jones, T.A., Cole, S.T., 2012. Structure and function of the transketolase from mycobacterium tuberculosis and comparison with the human enzyme. Open Biol. 2, 110026.

Gadau, S., Emanueli, C., Van Linthout, S., Graiani, G., Todaro, M., Meloni, M., Campesi, I., Invernici, G., Spillmann, F., Ward, K., Madeddu, P., 2006. Benfotiamine accelerates the healing of ischaemic diabetic limbs in mice through protein kinase B/Akt-mediated potentiation of angiogenesis and inhibition of apoptosis. Diabetologia 49, 405–420.

Hamaker, H.C., 1958. On hemacytometer counts. Biometrics 14, 558–559.

Hammes, H.P., Du, X., Edelstein, D., Taguchi, T., Matsumura, T., Ju, Q., Lin, J., Bierhaus, A., Nawroth, P., Hannak, D., Neumaier, M., Bergfeld, R., Giardino, I., Brownlee, M., 2003. Benfotiamine blocks three major pathways of hyperglycemic damage and prevents experimental diabetic retinopathy. Nat. Med. 9, 294–299.

Han, C., Lu, Y., Wei, Y., Liu, Y., He, R., 2011. D-ribose induces cellular protein glycation and impairs mouse spatial cognition. PLoS One 6, e24623.

Han, C., Lu, Y., Wei, Y., Wu, B., Liu, Y., He, R., 2014. D-ribosylation induces cognitive impairment through RAGE-dependent astrocytic inflammation. Cell Death Dis. 5, e1117.

Huang, R., Abdelmoneim, S.S., Nhola, L.F., Basu, R., Basu, A., Mulvagh, S.L., 2015. Relationship between glycosylated hemoglobin A1c and coronary flow reserve in patients with type 2 diabetes mellitus. Expert. Rev. Cardiovasc. Ther. 13, 445–453.

Huisman, T.H., Martis, E.A., Dozy, A., 1958. Chromatography of hemoglobin types on carboxymethylcellulose. J. Lab. Clin. Med. 52, 312–327.

Kashiwagi, A., Kasuga, M., Araki, E., Oka, Y., Hanafusa, T., Ito, H., Tominaga, M., Oikawa, S., Noda, M., Kawamura, T., Sanke, T., Namba, M., Hashiramoto, M., Sasahara, T., Nishio, Y., Kuwa, K., Ueki, K., Takei, I., Umemoto, M., Murakami, M., Yamakado, M., Yatomi, Y., Ohashi, H., 2012. International clinical harmonization of glycated hemoglobin in Japan: from Japan diabetes society to National Glycohemoglobin Standardization Program values. J. Diabetes Investig. 3, 39–40.

Kawaguchi, M., Koshimura, K., Murakami, Y., Kato, Y., 1999. Antihypertensive effect of insulin in the zucker diabetic fatty (ZDF) rat, an animal model for non-insulin dependent diabetes mellitus with insulin resistance. Biomed. Res. 20, 57–59.

Kim, Y., Kim, E.Y., Seo, Y.M., Yoon, T.K., Lee, W.S., Lee, K.A., 2012. Function of the pentose phosphate pathway and its key enzyme, transketolase, in the regulation of the meiotic cell cycle in oocytes. Clin. Exp. Reprod. Med. 39, 58–67.

Koenig, R.J., Peterson, C.M., Jones, R.L., Saudek, C., Lehrman, M., Cerami, A., 1976. Correlation of glucose regulation and hemoglobin AIc in diabetes mellitus. N. Engl. J. Med. 295, 417–420.

Leehey, D.J., Singh, A.K., Bast, J.P., Sethupathi, P., Singh, R., 2008. Glomerular renin angiotensin system in streptozotocin diabetic and zucker diabetic fatty rats. Transl. Res. 151, 208–216.

Liu, L., Hood, S., Wang, Y., Bezverkov, R., Dou, C., Datta, A., Yuan, C., 2008. Direct enzymatic assay for % HbA1c in human whole blood samples. Clin. Biochem. 41, 576–583.

Lonsdale, D., 2015. Thiamine and magnesium deficiencies: keys to disease. Med. Hypotheses 84, 129–134.

Lopez-Clavijo, A.F., Duque-Daza, C.A., Romero Canelon, I., Barrow, M.P., Kilgour, D., Rabbani, N., Thornalley, P.J., O'connor, P.B., 2014. Study of an unusual advanced glycation end-product (AGE) derived from glyoxal using mass spectrometry. J. Am. Soc. Mass Spectrom. 25, 673–683.

Makris, K., Spanou, L., 2011. Is there a relationship between mean blood glucose and glycated hemoglobin? J. Diabetes Sci. Technol. 5, 1572–1583.

Matsushika, A., Goshima, T., Fujii, T., Inoue, H., Sawayama, S., Yano, S., 2012. Characterization of non-oxidative transaldolase and transketolase enzymes in the pentose phosphate pathway with regard to xylose utilization by recombinant Saccharomyces cerevisiae. Enzym. Microb. Technol. 51, 16–25.

Michalak, S., Michalowska-Wender, G., Adamcewicz, G., Wender, M.B., 2013. Erythrocyte transketolase activity in patients with diabetic and alcoholic neuropathies. Folia Neuropathol. 51, 222–226.

Mul, J.D., Begg, D.P., Alsters, S.I.M., Van Haaften, G., Duran, K.J., D'alessio, D.A., Le Roux, C.W., Woods, S.C., Sandoval, D.A., Blakemore, A.I.F., Cuppen, E., Van Haelst, M.M., Seeley, R.J., 2012. Effect of vertical sleeve gastrectomy in melanocortin receptor 4-deficient rats. Am. J. Physiol.-Endocrinol. Metabol. 303, E103–E110.

Nathan, D.M., 1993. Long-term complications of diabetes mellitus. N. Engl. J. Med. 328, 1676–1685.

Pold, R., Jensen, L.S., Jessen, N., Buhl, E.S., Schmitz, O., Flyvbjerg, A., Fujii, N., Goodyear, L.J., Gotfredsen, C.F., Brand, C.L., Lund, S., 2005. Long-term AICAR administration and exercise prevents diabetes in ZDF rats. Diabetes 54, 928–934.

Reaven, G.M., 1988. Banting lecture 1988. Role of insulin resistance in human disease. Diabetes 37, 1595–1607.

Schaaffgerstenschlager, I., Zimmermann, F.K., 1993. Pentose-phosphate pathway in Saccharomyces-cerevisiae - analysis of deletion mutants for transketolase, transaldolase, and glucose-6-phosphate-dehydrogenase. Curr. Genet. 24, 373–376.

Seuffer, R., 1977. A new method for the determination of sugars in cerebrospinal fluid (author's transl). J. Clin. Chem. Clin. Biochem. 15, 663–668.

Sherwani, S.I., Khan, H.A., Ekhzaimy, A., Masood, A., Sakharkar, M.K., 2016. Significance of HbA1c test in diagnosis and prognosis of diabetic patients. Biomark. Insights 11, 95–104.

Siwy, J., Zoja, C., Klein, J., Benigni, A., Mullen, W., Mayer, B., Mischak, H., Jankowski, J., Stevens, R., Vlahou, A., Kossida, S., Perco, P., Bahlmann, F.H., 2012. Evaluation of the zucker diabetic fatty (ZDF) rat as a model for human disease based on urinary peiptidomic profiles. PLoS One 7, e51334.

Somani, B.L., Sinha, R., Gupta, M.M., 1989. Fructosamine assay modified for the estimation of glycated hemoglobin. Clin. Chem. 35, 497.

Stirban, A., Negrean, M., Stratmann, B., Gawlowski, T., Horstmann, T., Gotting, C., Kleesiek, K., Mueller-Roesel, M., Koschinsky, T., Uribarri, J., Vlassara, H., Tschoepe, D., 2006. Benfotiamine prevents macro- and microvascular endothelial dysfunction and oxidative stress following a meal rich in advanced glycation end products in individuals with type 2 diabetes. Diabetes Care 29, 2064–2071.

Stirban, A., Nandrean, S., Kirana, S., Gotting, C., Veresiu, I.A., Tschoepe, D., 2012. Benfotiamine counteracts smoking-induced vascular dysfunction in healthy smokers. Int. J. Vasc. Med. 2012, 968761.

Su, T., He, R., 2014. D-ribose, an overlooked player in type 2 diabetes mellitus? Sci. China Life Sci. 57, 361.

Su, T., He, R.Q., 2015. An insight of D-ribose metabolic imbalance in type 2 diabetes mellitus. Prog. Biochem. Biophys. 42, 390–392.

Su, T., Xin, L., He, Y.-G., Wei, Y., Song, Y.-X., Li, W.-W., Wang, X.-M., He, R.-Q., 2013. The abnormally high level of uric D-ribose for Type-2 diabetics. Prog. Biochem. Biophys. 40, 816–825.

Tarallo, S., Beltramo, E., Berrone, E., Porta, M., 2012. Human pericyte-endothelial cell interactions in co-culture models mimicking the diabetic retinal microvascular environment. Acta Diabetol. 49 (Suppl. 1), S141–51.

Tessier, F.J., Niquet-Leridon, C., Jacolot, P., Jouquand, C., Genin, M., Schmidt, A.M., Grossin, N., Boulanger, E., 2016. Quantitative assessment of organ distribution of dietary protein-bound 13 C-labeled Nvarepsilon -carboxymethyllysine after a chronic oral exposure in mice. Mol. Nutr. Food Res. 60, 2446–2456.

Trujillo, J., King, M., Mcdermott, M., 2013. Evaluation of initial management of severe hyperglycemia in T2DM. Diabetes 62, A652.

Tsou, C.L., 1962. Relation between modification of functional groups of proteins and their biological activity. I.A graphical method for the determination of the number and type of essential groups. Sci. Sinica 11, 1535–1558.

Van Putten, L.M., 1958. The life span of red cells in the rat and the mouse as determined by labeling with DFP32 in vivo. Blood 13, 789–794.

Warhurst, D.C., Williams, J.E., 1996. ACP broadsheet no 148. July 1996. Laboratory diagnosis of malaria. J. Clin. Pathol. 49, 533–538.

Wei, Y., Chen, L., Chen, J., Ge, L., He, R.Q., 2009. Rapid glycation with D-ribose induces globular amyloid-like aggregations of BSA with high cytotoxicity to SH-SY5Y cells. BMC Cell Biol. 10, 10.

Wei, Y., Han, C.S., Zhou, J., Liu, Y., Chen, L., He, R.Q., 2012. D-ribose in glycation and protein aggregation. Biochim. Biophys. Acta-Gen. Subj 1820, 488–494.

Wei, Y., Han, C., Wang, Y., Wu, B., Su, T., Liu, Y., He, R., 2015. Ribosylation triggering alzheimer's disease-like tau hyperphosphorylation via activation of CaMKII. Aging Cell 14, 754–763.

Weng, D., Lu, Y., Wei, Y., Liu, Y., Shen, P., 2007. The role of ROS in microcystin-LR-induced hepatocyte apoptosis and liver injury in mice. Toxicology 232, 15–23.

Weykamp, C.W., Mosca, A., Gillery, P., Panteghini, M., 2011. The analytical goals for hemoglobin A(1c) measurement in IFCC units and National Glycohemoglobin Standardization Program Units are different. Clin. Chem. 57, 1204–1206.

Wu, B., Wei, Y., Wang, Y., Su, T., Zhou, L., Liu, Y., He, R., 2015. Gavage of D-ribose induces Abeta-like deposits, Tau hyperphosphorylation as well as memory loss and anxiety-like behavior in mice. Oncotarget 6, 34128–34142.

Xu, Y.J., Wu, X.Q., Liu, W., Lin, X.H., Chen, J.W., He, R.Q., 2002. A convenient assay of glycoserum by nitroblue tetrazolium with iodoacetamide. Clin. Chim. Acta 325, 127–131.

Yokoi, N., Hoshino, M., Hidaka, S., Yoshida, E., Beppu, M., Hoshikawa, R., Sudo, K., Kawada, A., Takagi, S., Seino, S., 2013. A novel rat model of type 2 diabetes: the Zucker Fatty Diabetes Mellitus ZFDM rat. J. Diabetes Res. 2013, 103731.

Zhao, J., Zhong, C.J., 2009. A review on research progress of transketolase. Neurosci. Bull. 25, 94–99.